

Design Principles for Supercritical CO₂ Viscosifiers

Stephen Cummings^a, Dazun Xing^b, Robert Enick^b, Sarah Rogers^c, Richard Heenan^c, Isabelle Grillo^d and Julian Eastoe^{a*}

^a School of Chemistry, University of Bristol, Cantock's Close, Bristol, BS8 1TS, UK

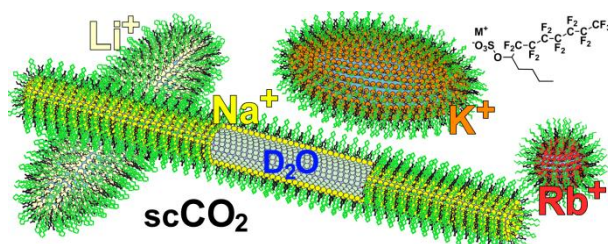
E-mail: Julian.Eastoe@bristol.ac.uk

^b National Energy Technology Laboratory IAES, and Department of Chemical and Petroleum Engineering, Swanson School of Engineering University of Pittsburgh, 3700 O'Hara Street, Pittsburgh PA 15261, USA

^c ISIS-CCLRC, Rutherford Appleton Laboratory, Chilton, Oxon OX11 0QX, U.K

^d Institut Max-von-Laue-Paul-Langevin, BP 156-X, F-38042 Grenoble Cedex, France,

By varying the F7H4 surfactant counterion hydrated radius, it has been possible to create a range of non-spherical micelle architectures in supercritical CO₂ (scCO₂), which enhance viscosity. Furthermore this array of morphologies can be related to measurements performed at the air-water interface.



Surfactant Synthesis:

Synthesis of the Grignard N-butylmagnesium Bromide:

The reaction was performed under N₂. A few drops of 1-bromobutane (total quantity 35 cm³, 330 mmol, held in a dropping funnel) were added to a dispersion of magnesium turnings, with a single crystal of iodine, in 100 ml of diethyl ether. The reaction was gently activated by means of a hot-air gun, and weak effervescence was observed at the magnesium surface, with further addition of bromobutane the reaction accelerated, with white flocculation appearing in the solution and ether starting to reflux. At this stage the remaining bromobutane was diluted with 30 cm³ of diethyl ether, and added slowly over a half hour or so. Once the addition of bromobutane was completed the reaction mixture was refluxed at 50 °C for 2 and half hours. After this the reaction was cooled to room temperature and allowed to settle down.

Synthesis of the pentadecafluoro-5-dodecanone:

The reaction was performed under N₂. A 250 cm³ pressure equalising dropping funnel containing a solution of pentadecafluorooctanoic acid in 100 cm³ of diethyl ether was fitted to the apparatus mentioned above. The solution was then added drop-wise over an hour at room temperature to the previously formed Grignard reagent whilst stirring. After refluxing the reaction mixture for 4 and half hours, the reaction was then cooled down to 0 °C, and acidified with 200 cm³ of 10% HCl solution. Excess magnesium was then filtered off, the upper yellow organic phase separated, whilst the lower aqueous phase was extracted with diethyl ether (3 × 50 cm³). All ether extracts were combined and washed with saturated aqueous solution of sodium hydrogen carbonate (2 × 75 cm³) and saturated aqueous solution of sodium chloride. The resulting organic phase was then dried over magnesium sulfate. The remaining solvent was then rotary evaporated, with resulting yellow oil then being vacuum distilled to high purity to give a light yellow colored oil.

Synthesis of the pentadecafluoro-5-dodecanol:

Sodium borohydride (3.5g, 91 mmol, 1.15 equiv.) was added portion-wise to a solution of ketone (40g 79 mmol, 1.0 equiv) in 300 cm³ of ethanol at 0 °C whilst stirring. The reaction was left for 3 hours at

0 °C and then for one hour at room temperature. At the end of the reaction most of solvent was evaporated and the resulting mixture was neutralised at 0 °C with 50% acetic acid solution. With aid of ethanol water was removed by rotary evaporation and the remaining solution was dissolved in 250 cm³ of diethyl ether. After repeated washing of the organic layer with water (1 × 50 cm³), sodium hydrogen carbonate (4 × 75 cm³), and with water again (2 × 50 cm³), the crude alcohol was obtained by rotary evaporation. Further water removal was achieved azeotropically by rotary evaporation with toluene. The alcohol product was a white oil which, on cooling, produced white crystals.

Synthesis of Sodium pentadecafluoro-5-dodecyl sulfate – F7H4:

Controlled addition at 0 °C of chlorosulfonic acid (9.0 cm³, 135 mmol, 1.9 equiv) to 60 cm³ of pyridine produced a white solid. A solution of pentadecafluoro-5-dodecanol in 55 cm³ of pyridine was added to this dispersion at 0 °C and with stirring,. The reaction mixture was slowly warmed to 60 °C until it turned transparent yellow (after ~ 1 hour). The reaction mixture was then quenched in ~600 cm³ of ice cooled, saturated sodium carbonate solution and left for 1 hour and half, allowing for sodium hydrogen carbonate salts to precipitate out. The said salts were filtered, and the product extracted with butanol (3 × 75 cm³). The aqueous layers were separated and the pyridine and butanol phases combined. Solvent evaporation yielded the crude surfactant, which was purified using a minimum amount of distilled dry acetone.

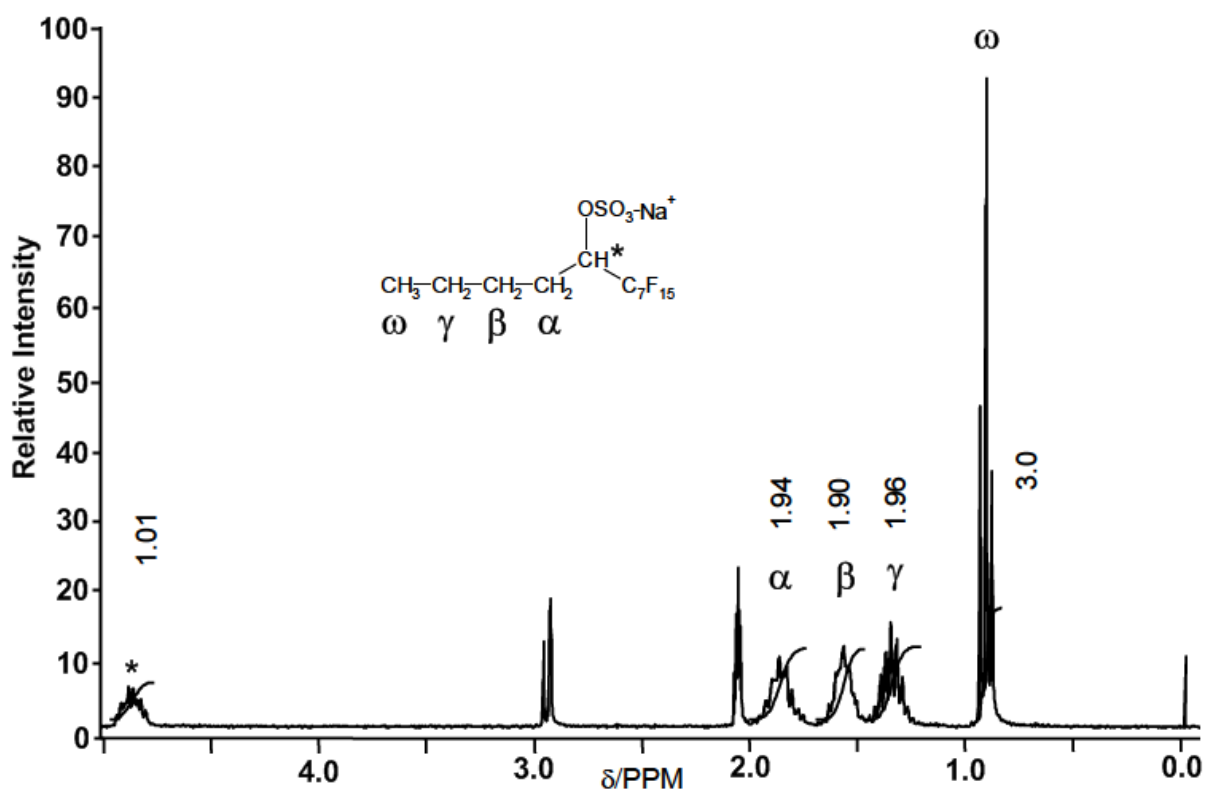


Figure S1: ^1H NMR of F7H4 and spectral assignments of M-F7H4

HP SANS using a custom-made pressure cell

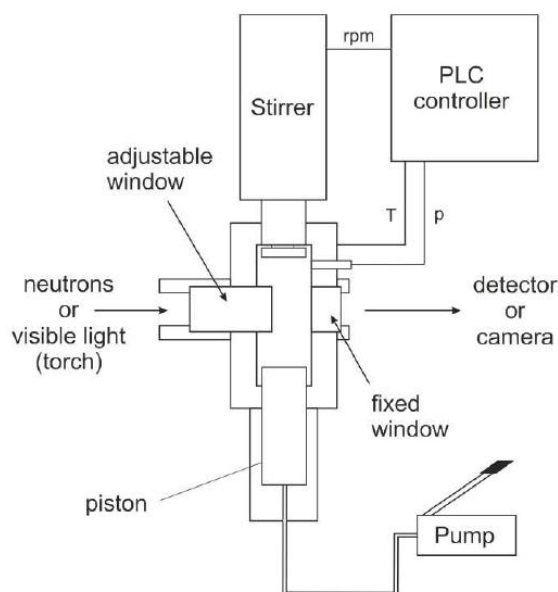


Figure S2: Schematic of the HP-SANS pressure cell system.

The SPM25 pressure cell was designed by Thar Technologies, Inc. (Thar Instruments, 575 Epsilon Drive, Pittsburgh, PA 15238) specifically for HP-SANS measurements in scCO_2 , based on a commercially available SPM20 unit. The cell incorporates two sapphire windows mounted 180° to each other. Figure S1 shows a schematic diagram of the cell. The viewed diameter of the windows is 17.35 mm and the path length between the inside faces of the windows is adjustable (from 0 – 19 mm). With the top loaded magnetically coupled stirrer/propeller in place the maximum working pressure is 413 bar (5700 psia). Pressurised CO_2 is injected into the cell via a syringe pump; further pressure adjustments can be made via a movable piston driven by a hydraulic pump. Vessel pressure is detected by a transducer mounted in the side of the cell body. Both temperature and pressure are monitored remotely by a PLC controller, enabling remote adjustment of these parameters during neutron experiments.

Air-water surface tension behaviour of Na-F7H4.

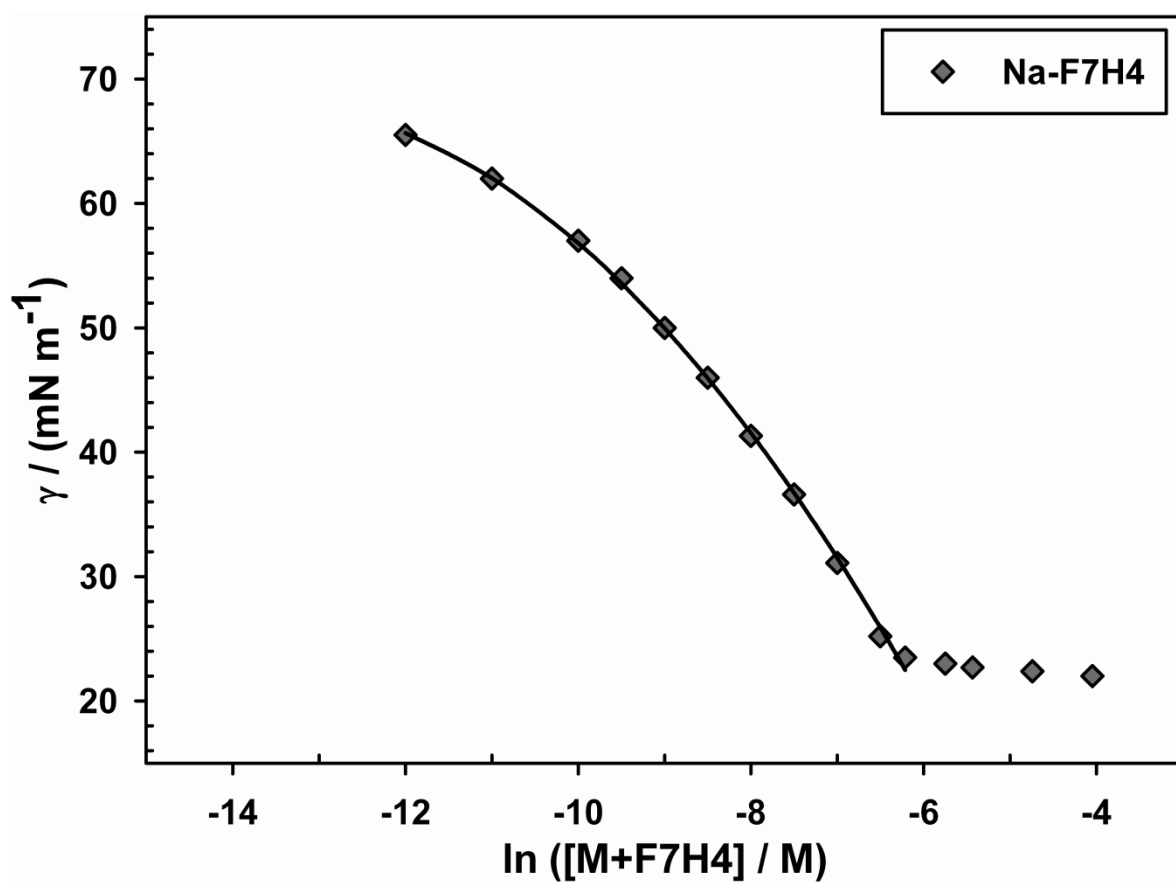


Figure S3: Surface tension curve for Na-F7H4 with a quadratic fit to the pre-cmc region.

SANS data fitting:

All SANS profiles were fitted using the interactive FISH program¹ written by R. K. Heenan, which employs a standard iterative least-squares method.

Spheres

The form factor for polydisperse spheres, each with radius R , is defined as follows²:

$$(1) \quad P(Q) = \int_0^{\frac{\pi}{2}} |G(Q, R)|^2 g(R) dR$$

$$(2) \quad G(Q, R) = \left(\frac{4\pi}{3}\right) R^3 \Delta\rho \left[\frac{3j_1(QR)}{QR} \right]$$

Where $j_1(QR)$ is a first order spherical Bessel function and $g(R)$ is (in this case) defines a Schultz distribution of homogeneous spheres:

$$(3) \quad g(R) = \frac{\left(\frac{Z+1}{\bar{R}}\right)^{Z+1} R^Z \exp\left[-\left(\frac{Z+1}{\bar{R}}\right)R\right]}{\Gamma(Z+1)}$$

Where the width parameter, $Z > -1$, \bar{R} is the mean of the distribution and polydispersity is defined by an RMS deviation $\sigma = \bar{R} / (Z+1)^{1/2}$. Parameters fit in FISH were sphere radius r_{D2O} , polydispersity index σ , and the Shultz scale factor given by $SF = 10^{-24} \varphi_{agg} (\Delta\rho)^2$ where φ_{agg} is the aggregate volume fraction and $\Delta\rho$ is the contrast step between solvent medium and surfactant aggregates. Using these calculated values, SANS fitting was carried out to fixed values of r and σ in order to obtain a value for φ_{agg} . Due to natural uncertainties in measured absolute intensity ($\pm 5\%$), the exact value for $\Delta\rho$, and also the recognized close coupling in the fitting models between scale factor and aggregate radius in polydisperse samples, this calculated φ_{agg} should only be treated as a guide.

Ellipsoids

The scattering law for ellipsoids of radii r_1 , r_2 and L with $L = X \times r$ (where X is the aspect ratio) is summarised in equations 4-6. It requires a numerical integration of $P(Q)$ over angle α .³

$$(4) \quad P(Q) = \int_0^{\frac{\pi}{2}} F^2[Q, \Phi(r, X, \alpha)] \sin \alpha d\alpha$$

$$(5) \quad \Phi(r, X, \alpha) = r(\sin^2 \alpha + X^2 \cos^2 \alpha)^{1/2}$$

$$(6) \quad V = \frac{4\pi X r_{D_2O}^3}{3}$$

Parameters fitted in FISH were ellipsoid cross section radius r_{D_2O} , axial ratio X and scale factor given by $n_p V^2 (\Delta\rho)^2$ where n_p is aggregate number density. Above an aspect ratio $X \sim 7$ the ellipsoid form factor tends to that for a rigid homogeneous cylinder (given below).

Cylinders

For N randomly oriented rods of length L and cross-sectional radius R , the form factor $P(Q)$ is given by 7-9 below.⁴

$$(7) \quad P(Q) = N \int_0^{\frac{\pi}{2}} F^2(Q) \sin(\gamma) d\gamma$$

$$(8) \quad F(Q) = (\Delta\rho)V \frac{\sin(\frac{1}{2}QL \cos \gamma)}{\frac{1}{2}QL \cos \gamma} \frac{2J_1(Qr \sin \gamma)}{Qr \sin \gamma}$$

$$(9) \quad V = \pi r_{D_2O}^2 L$$

$J_1(x)$ is the first order Bessel function of the first kind and integration is carried out numerically over angle γ between the Q vector and the axis of the rod. Parameters fitted in FISH were D_2O radius r_{D_2O} , rod length L and the scale factor given by $10^{-24} \phi (\Delta\rho)^2$ where ϕ is aggregate volume fraction and $\Delta\rho$ is the contrast step (known).

Structure factor $S(Q)$ for F7H4 in D₂O

Surfactant	r_{F7H4}	R_{F7H4}	X	t_{F7H4}	$S(Q)$	Charge q	AKK
Li-F7H4	15.7	-	-	-	26.21 Hayter Penfold	14.0	0.081
Na-F7H4	15.9	-	-	-	3.26 Hayter Penfold	12.0	0.080
K-F7H4	16.5	38	2.3	-	23.56 Hayter Penfold	20.0	0.078
Rb-F7H4	234	-	-	28.2	0.0313 Hard Sphere	-	0.075

Table S1: Structural parameters for F7H4-D₂O systems including $S(Q)$ contributions and type, and the charge and AKK used in these models.

Phase stability of Na-F7H4 scCO₂ systems:

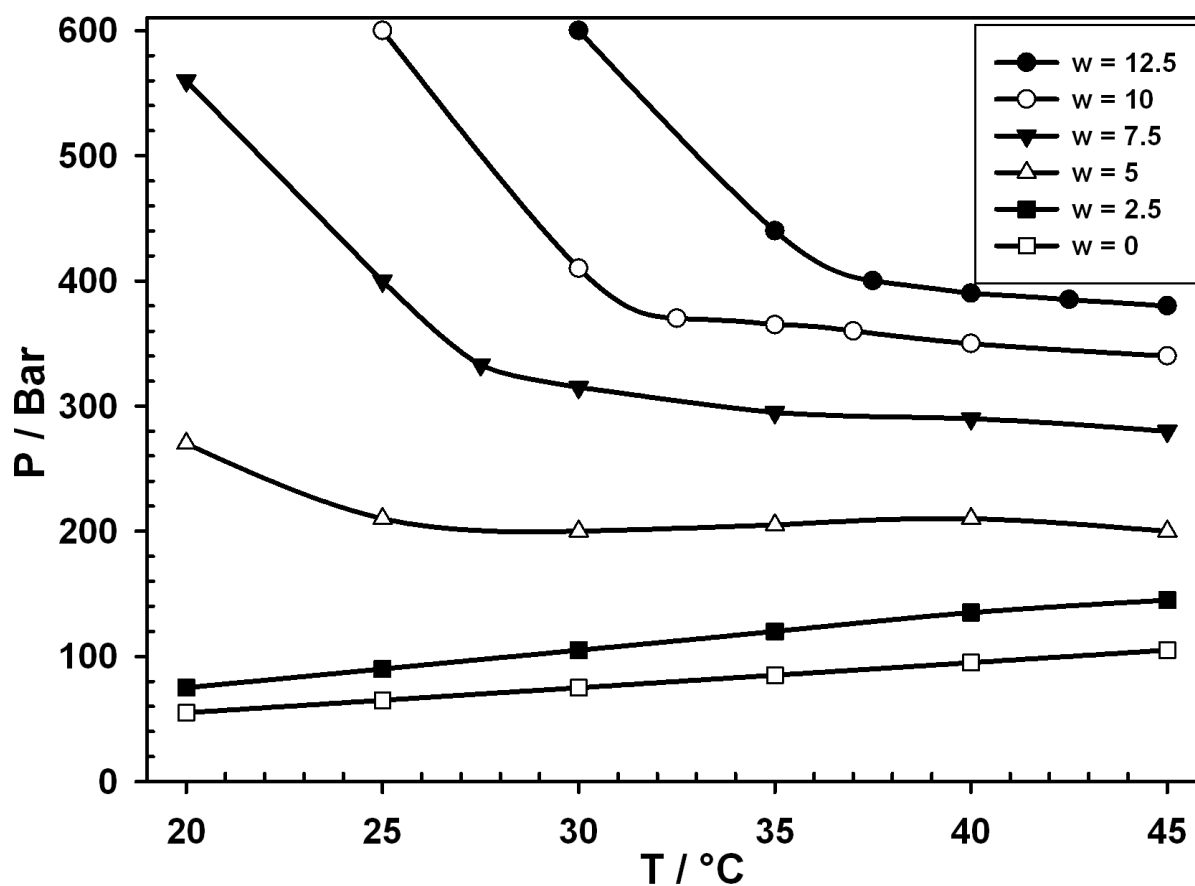


Figure S4: Pressure-temperature phase diagrams of w/c microemulsion systems for Na-F7H4 in scCO₂ with water content, $w = [H_2O]/[surfactant]$.

Small Angle Neutron Scattering (SANS) of F7H4-scCO₂ systems

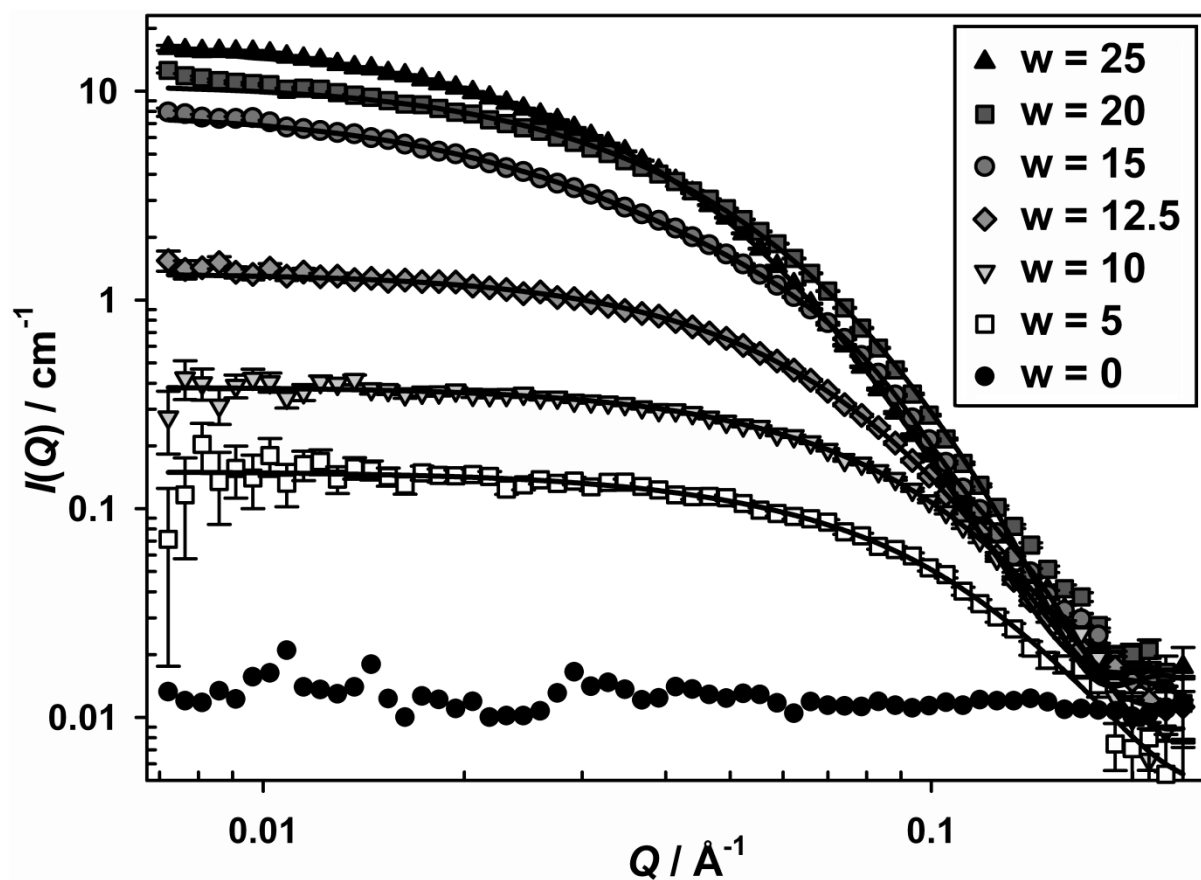


Figure S5: HP-SANS profiles for w/c microemulsion systems of K-F7H4, at 4.4 wt% in scCO₂ at 400 bar, 40 °C ($w = [\text{D}_2\text{O}]/[\text{surfactant}]$). Fitted scattering laws are shown as lines with derived parameters listed in Table 3 (main paper).

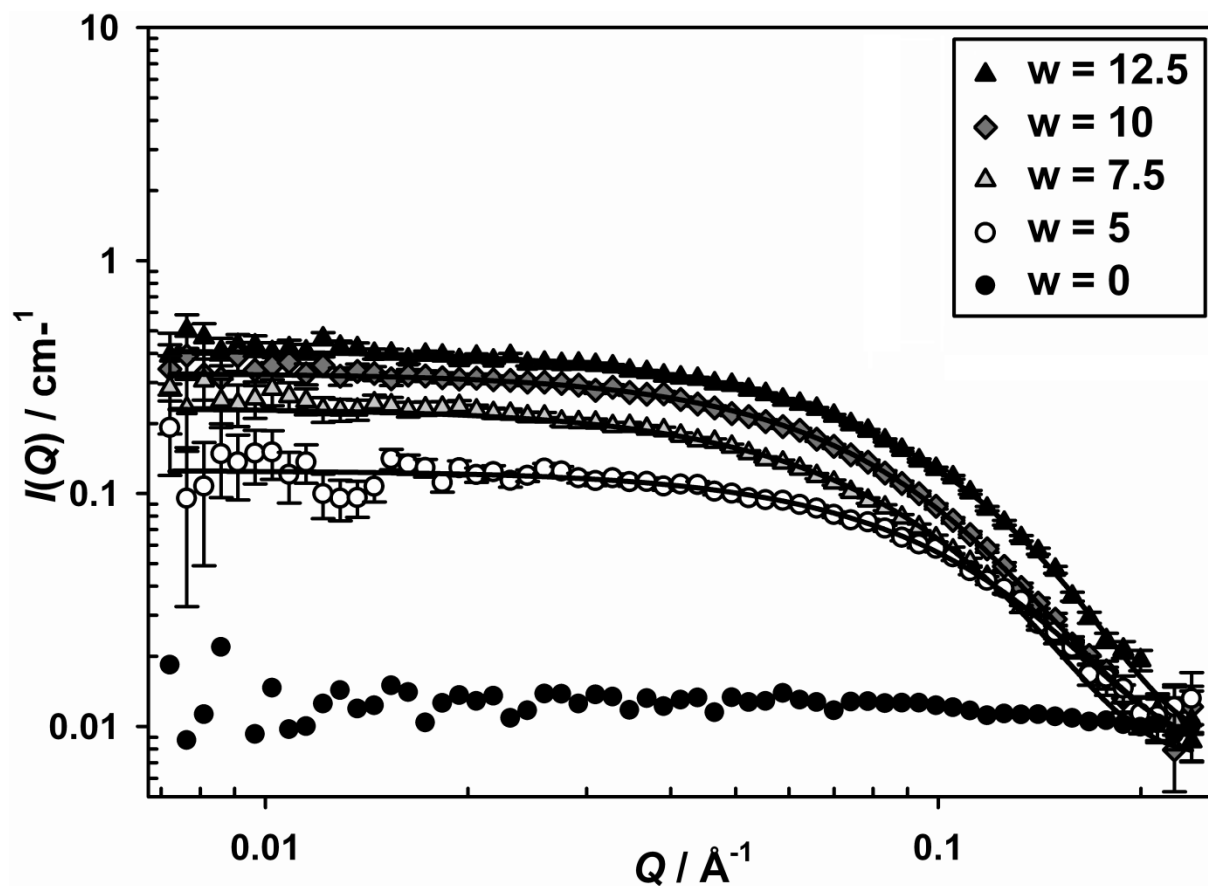


Figure S6: HP-SANS profiles for w/c microemulsion systems of Rb-F7H4, at 4.4 wt% in scCO₂ at 400 bar, 40 °C ($w = [\text{D}_2\text{O}]/[\text{surfactant}]$). Fitted scattering laws are shown as lines with derived parameters listed in Table 3 (main paper).

High pressure Viscometry

Relative viscosity can be estimated by⁵:

$$(10) \quad \frac{\eta_{\text{mic}}}{\eta_{\text{CO}_2}} \cong \eta_{\text{rel}} \cong 1 + [\eta]\phi_p + K_H[\eta]^2\phi_p^2$$

Where K_H ⁵:

$$(11) \quad K_H \cong \frac{2}{5}(1 - 0.00142Pe_{\text{rot}}^2)$$

With Pe_{rot} ² being described by⁵:

$$(12) \quad Pe_{\text{rot}} = \frac{\dot{\gamma}}{D_{\text{rot}}}$$

Where $\dot{\gamma}$ is the shear rate ($\sim 11000 \text{ s}^{-1}$) and D_{rot} is the rotational diffusion coefficient^{6,7}:

$$D_{\text{rot}} = \frac{3kT}{\pi\eta_0 L^3} \left[\ln\left(\frac{2L}{d}\right) - 0.5(\gamma_{\parallel} + \gamma_{\perp}) \right]$$

(13)

Where γ_{\parallel} and γ_{\perp} are the particle end-effect corrections and the validity of these expressions holds for different ranges of the aspect ratio. The expressions used here are those of Tirado et al.⁸, which are valid for aspect ratios in the range of $2 < L/d (X) < 30$.

$$\gamma_{\parallel} = -0.114 - \frac{0.15}{\ln 2X} - \frac{13.5}{(\ln 2X)^2} + \frac{37}{(\ln 2X)^3} - \frac{22}{(\ln 2X)^4}$$

$$\gamma_{\perp} = 0.866 - \frac{0.15}{\ln 2X} - \frac{8.1}{(\ln 2X)^2} + \frac{18}{(\ln 2X)^3} - \frac{9}{(\ln 2X)^4}$$

CO₂ neat viscosity, $\eta_0 = 0.00011 \text{ Pa s}^{9,10}$

Species	w	Aspect Ratio, X_{mic}	$\eta_{\text{mic}}/\eta_{\text{CO}_2}$	Intrinsic viscosity, $[\eta]$	Calc η_{rel}	$D_{\text{rot}} / \text{s}^{-1}$	Pe_{rot}	K_{H}
Li-F7H4	15. 0	4.2	1.18	4.9	1.24	3888367	0.002828951	0.4
Na-F7H4	12. 5	10.5	1.76	14.6	1.82	696168	0.01580078	0.4
K-F7H4	15. 0	3.0	1.11	3.8	1.18	4146457	0.002652867	0.4

References

- (1) Heenan, R. K. *Rutherford Appleton Laboratory Report* Rutherford Appleton Laboratory, 1989.
- (2) Kotlarchyk, M.; Chen, S.-H. *The Journal of Chemical Physics* **1983**, *79*, 2461.
- (3) Guinier, A. *Ann. Phys.* **1939**, *12*, 161.
- (4) Fournet, G. *Bull. Soc. Fr. Mineral. Crist.* **1951**, *74*, 37.
- (5) Wierenga, A. M.; Philipse, A. P. *Colloids Surf., A* **1998**, *137*, 355.
- (6) Lehner, D.; Lindner, H.; Glatter, O. *Langmuir* **2000**, *16*, 1689.
- (7) Broersma, S. *The Journal of Chemical Physics* **1960**, *32*, 1626.
- (8) Tirado, M. M.; Martinez, C. L.; Torre, J. G. d. l. *The Journal of Chemical Physics* **1984**, *81*, 2047.
- (9) Fenghour, A.; Wakeham, W. A.; Vesovic, V. *Journal of Physical and Chemical Reference Data* **1998**, *27*, 31.
- (10) Xiong, Y.; Kiran, E. *Polymer* **1995**, *36*, 4817.